

Chapter 2

Delay System Modeling of Rotary Drilling Vibrations

Islam Boussaada, Belem Saldivar, Hugues Mounier, Sabine Mondié, Arben Cela and Silviu-Iulian Niculescu

Abstract Vibrations in rotary drilling systems are oscillations occurring without being intentionally provoked. They often have detrimental effects on the system performance and are important source of economic losses; drill bit wear, pipes disconnection, borehole disruption and prolonged drilling time. By this chapter, we provide an improved modeling for the rotary drilling system. Among others, the proposed modeling takes into account; the infinite dimensional settings of problem as well as the nonlinear interconnected dynamics.

I. Boussaada (✉)

IPSA and Laboratoire des Signaux et Systèmes, CNRS-CentraleSupélec-Université Paris-Sud,
3 Rue Joliot-Curie, 91192 Gif-sur-Yvette, cedex, France
e-mail: islam.boussaada@lss.supelec.fr

B. Saldivar

Laboratoire des Signaux et Systèmes, Supélec-CNRS-UPSUD,
3 Rue Joliot-Curie, 91192 Gif-sur-Yvette, cedex, France
e-mail: belem.saldivar@lss.supelec.fr

H. Mounier

Laboratoire des Signaux et Systèmes, Université Paris-Sud-CNRS-CentraleSupélec,
3 Rue Joliot-Curie, 91192 Gif-sur-Yvette, cedex, France
e-mail: hugues.mounier@lss.supelec.fr

S. Mondié

Department of Automatic Control, CINVESTAV, Mexico City, Mexico
e-mail: smondie@ctrl.cinvestav.mx

A. Cela

Department of Computer Science and Telecommunication, UPE, ESIEE Paris, 93162
Noisy-Le-Grand, France
e-mail: celaa@esiee.fr

S.-I. Niculescu

Laboratoire des Signaux et Systèmes, CNRS-CentraleSupélec-Université Paris-Sud,
3 Rue Joliot-Curie, 91192 Gif-sur-Yvette, cedex, France
e-mail: Silviu.Niculescu@lss.supelec.fr

2.1 Introduction

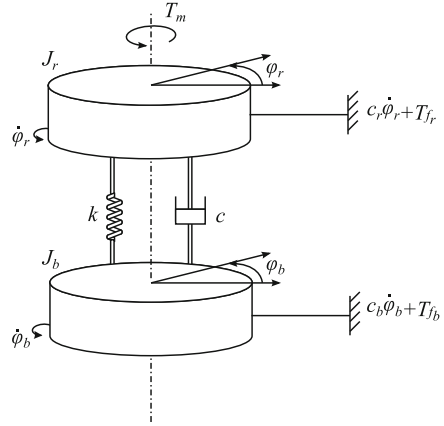
A rotary drilling structure is mainly composed of a rig, a drillstring, and a bit. In oil well drilling operations, one of the most important problem to deal with consists in suppressing harmful vibrations yielding to stick-slip and bit-bouncing oscillations. Indeed, these undesired dynamics can cause various damages such as pipes and bit break. This spoilage has a leaden economical effect. The drilling control failure is mainly due to poor modeling and/or control. This chapter focuses on the modeling task upon which the analysis and control rely on. The modeling must entail two aspects. The first one, “physics dynamics”, consists in describing the motions equations of the phenomena occurring during the drilling process. The second, “sensing and transmission model”, amounts to write down equations allowing to obtain informations on the bit state, an essential information to overcome the above mentioned problems. Unfortunately, this information is degraded and/or delayed, due to technological constraints. In this chapter, we are concerned solely by physical modeling, yet, we are taking into account transmission in deriving an overall system’s model. In the literature, one may find several types of models ranging from partial differential equations to ordinary differential equation ones with one or several degrees of freedom representing the dynamics of drilling systems. This contribution is organized as follows: In the first section, we report the most relevant works concerned by the physical modeling of the drilling vibrations. The second section is devoted to present the PDE model that we build to account for axial and torsional vibrations. The proposed model improves the known models since it addresses several critical issues that arise when the latter are considered. The chapter is completed by insights on Wireless sensing transmission models, as well as on actuating and related motor types. Finally, we derive a model covering most of the dynamics needed to be taken into account for control purposes. The chapter ends with some comments in wireless-transmission and real-time control methodology.

2.2 State of the Art

To the best of the authors’ knowledge, torsional drilling vibrations have received much more attention compared to axial vibrations.

As underlined in [41], the simplest approximation consists in neglecting the effects of the axial and lateral vibrations and in ignoring the finite propagation time of torsional waves along the drillstring. The model turns to be a simple forced torsional pendulum under nonlinear damping at the bit. Thus, the full spectrum of the torsional vibrations is replaced by a simple torsional spring that couples the torque Φ_{top} from the top-drive with the torque Φ_{bit} generated in the bit/rock interface. Such an approximation leads to the following coupled system model

Fig. 2.1 Drill string two-coupled masses model



$$\begin{cases} \ddot{\Phi}_{top} + G_{top}(\Phi_{top} - \Phi_{bit}) = T_{motor}(\Phi_{top}, \Phi_{bit}, \dot{\Phi}_{top}, t), \\ \ddot{\Phi}_{bit} + G_{bit}(\Phi_{bit} - \Phi_{top}) = -\mathcal{F}(\dot{\Phi}_{bit}), \end{cases} \quad (2.1)$$

where \mathcal{F} designates the bit-torque friction, G_{bit} G_{top} are the coupling physical constants, $G_{top} = G/\rho$ is some positive constant proportional to the torsional rigidity of the drillstring, $G_{bit} = G J_{top}/J_{bit}$ and T_{motor} is the top control torque. Here G denotes the shear modulus of drilling steel, ρ is the steel density, J_{top} and J_{bit} are respectively the inertia moment of a pipe section and the inertia moment of the drill collar section.

In [3], the drillstring system is modeled as two coupled masses as shown in Fig. 2.1. J_{top} and J_{bit} are two inertial masses locally damped by d_{top} and d_{bit} . The inertias are coupled through an elastic shaft of stiffness k and damping c . Let us define Φ_{top} , Φ_{bit} as the angular positions of the rotary and the bit respectively; $\dot{\Phi}_{top}$, $\dot{\Phi}_{bit}$ as their angular velocities, $u(t) = W o B$ is the weight on the bit control signal, $v(t)$ is the rotary table torque control signal used to regulate $\dot{\Phi}_{top}$, μ is the friction coefficient; A , B , H , C_o are model matrices given in (2.4), $\Psi(t) = \Psi(u(t)) = H u(t)$, x is the state vector and y_o is the output variable. For a more detailed description, see, for instance, [8]. With the above notations, the model is represented as follows:

$$\begin{aligned} \dot{x}(t) &= A x(t) + B v(t) + \Psi(t) \mu \\ y_o &= C_o x = \dot{\Phi}_{top}, \end{aligned} \quad (2.2)$$

where the state $x = [x_1 \ x_2 \ x_3]^T$ is defined as follows:

$$x_1 = \Phi_{top} - \Phi_{bit}, \quad x_2 = \dot{\Phi}_{top}, \quad x_3 = \dot{\Phi}_{bit} \quad (2.3)$$

and

$$A = \begin{pmatrix} 0 & 1 & -1 \\ -\frac{k}{J_{top}} - \frac{d_{top}+c}{J_{top}} & \frac{c}{J_{top}} & \frac{c}{J_{top}} \\ \frac{k}{J_{bit}} & \frac{c}{J_{bit}} & -\frac{c+d_{bit}}{J_{bit}} \end{pmatrix}, \quad B = \begin{pmatrix} 0 \\ \frac{1}{J_{top}} \\ 0 \end{pmatrix}$$

$$H = \begin{pmatrix} 0 \\ 0 \\ -\frac{1}{J_{bit}} \end{pmatrix}, \quad C_o = (0 \ 1 \ 0) \quad (2.4)$$

In [30], a piecewise-smooth model of three degrees of freedom, which exhibits friction-induced stick-slip oscillations, is considered in order to describe a simplified torsional lumped-parameter model of an oilwell drillstring. In [28] a piecewise finite dimensional multi degree of freedom (multi DOF) model is considered for describing the torsional motion. In [29], a more general nonlinear differential equation-based model of a drillstring is analyzed. The aim of the proposed drillstring model is to avoid simulation problems due to the discontinuities originated by dry friction. Namely, the system of ordinary differential equations

$$\dot{x}(t) = Ax(t) + Bu(t) + T_f(x(t)), \quad (2.5)$$

where $x(t)$ is the state, A and B are constant matrices of appropriate dimension and T_f is the torque on bit. In [28], the authors reproduce stick-slip vibrations under different operating conditions. The model used for the torque on the bit is the main difference with respect to other models proposed in the literature. In [27], a discontinuous lumped parameter torsional model of four degrees of freedom is considered. This model allows to describe drill pipes and drill collars behavior. The closed-loop system has two discontinuity surfaces where one of them gives rise to self-excited bit stick-slip oscillations and bit sticking phenomena.

Several PDE models were introduced in the literature for specific describing torsional vibrations. For instance, in [2], torsional vibrations are modeled by a wave equation and the stick-slip dynamics are numerically characterized. In [35] a similar model is studied and a flatness-based approach that avoids such undesired dynamics is introduced. In [37, 38], a wave equation model to reproduce torsional drilling dynamics is proposed, this model is coupled to a damped harmonic oscillator model described by an ODE to approximate the longitudinal dynamics of the drilling system. In [33] as well as in [19] a nonlinear analytical study is introduced for the case of simple nonlinearities that occurs for a simplified frictional weight and torque which are proportional to $1 + \text{sign}(dU/dt)$ where U denotes the axial vibration. This model corresponds to a simplified torsional lumped-parameter model of an oilwell drillstring. An alternative method to characterize the stick-slip motion and other bit-sticking problems in such a drilling system is proposed. The method is based on the study of the relationships between the different types of system equilibria and the existing sliding motion when the bit velocity is zero. It is shown that such a sliding motion plays a key role in the presence of non-desired bit oscillations and transitions.

Furthermore, a proportional-integral-type controller is designed in order to drive the rotary velocities to a desired value. The ranges of the controller and the system parameters which lead to a closed-loop system without bit-sticking phenomena are identified.

Unfortunately, the models considered in [27–30] are linear ones, a quite crude approximation to the nonlinearities of the drillstring system leading to impoverish the possible dynamics. Moreover, the friction torque is always considered as a piecewise linear function of the state, which can be improved by the friction law that we are discussing in some of the following paragraphs.

2.3 Wave Equation Modelling

We consider a solid homogeneous metal flexible bar of length L and of section σ_0 . We are concerned by axial vibrations. Let $q(x, t)$ be the displacement at time t of a point x of the bar with respect to its equilibrium position. Let $T(x, t)$ be the tension applied on the bar at the point x at time t .

The *fundamental elasticity law* establishes a relation between the elongation $dl := l - l_0$ and the infinitesimal tension $dT := T - T_0$ (where we consider an element of length l_0 under the mean tension T_0) by:

$$\frac{dT}{\sigma_0} = E_0 \frac{dl}{l_0}, \quad (2.6)$$

where E_0 designates the Young modulus, or elasticity factor under the tension T_0 . This law can be applied only for a sufficiently small relative elongation dl/l_0 . Since at time t , the segment $(x, x + \Delta x)$ is of static length l_0 and occupies the position $(x + q(x, t), x + \Delta x + q(x + \Delta x, t))$. The length of the segment passes from $l_0 = \Delta x$ to $l = l_0 + dl = \Delta x + \partial_x q \Delta x$, we then have $\frac{dl}{l_0} = \partial_x q$, and the elasticity law implies:

$$T - T_0 = E_0 \sigma_0 \partial_x q. \quad (2.7)$$

Let ρ_0 be the linear density at the equilibrium of the bar (that is the rate of mass per a length unit). The fundamental principle of dynamics reads $\rho_0 \partial_t^2 q \Delta x = \partial_x T \Delta x$, by using (2.7) we have

$$\rho_0 \partial_t^2 q = E_0 \sigma_0 \partial_x^2 q, \quad (2.8)$$

which is a wave equation with speed $v = \sqrt{\frac{E_0 \sigma_0}{\rho_0}}$.

The axial vibrations of a solid bar constitute the essential of the sound propagation phenomena. The obtained model can be normalized, yielding to:

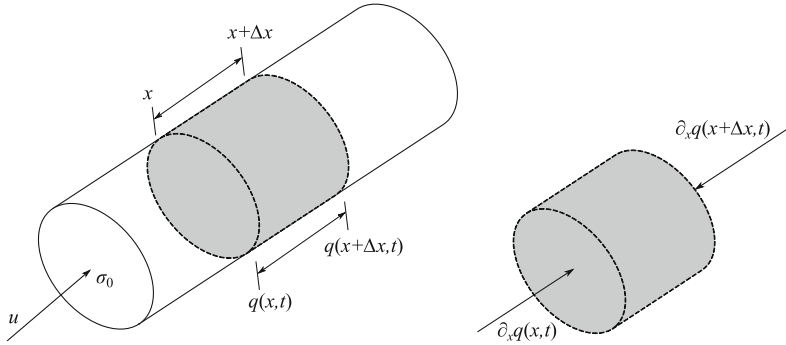


Fig. 2.2 (Left) Flexible bar, (Right) tension applied in a short segment of the bar

$$\partial_t^2 q(x, t) = \partial_x^2 q(x, t) \quad (2.9a)$$

$$\partial_x q(0, t) = -u(t) \quad \partial_x q(1, t) = 0 \quad (2.9b)$$

$$q(x, 0) = q_0(x) \quad \partial_t q(x, 0) = q_{t_0}(x) \quad (2.9c)$$

where $x \in [0, 1]$. The equation (2.9a) is the normalized wave equation (2.8) where (2.9b) is the boundary condition and (2.9c) is the initial equation. By Eqs.(2.7) and (2.9b), one can see that we apply a control law at the point $x = 0$ and no tension is applied on the free end ($x = 1$) (Fig. 2.2).

2.4 PDE Models

The lumped parameter model of the drillstring described in [2] consists of an angular pendulum of stiffness C ended with a lumped inertia J and a mass M . The latter two are free to move axially and represent the BHA as a unique rigid body. At the top of the drillstring, an upward force H and a constant angular velocity Ω are imposed. It is assumed that the weight-on-bit provided by the drillstring to the bit $W_0 = W_s - H$ is constant, which implies that the hook load H is adjusted to compensate for the varying submerged weight of the drillstring W_s . More precisely, the authors describe the torsional motion of a driven drillstring by the following wave equation with boundary conditions:

$$\begin{cases} \partial_t^2 \Phi(t, s) = c^2 \partial_s^2 \Phi(t, s), \\ \partial_t \Phi(t, 0) = \Omega, \\ J \partial_t^2 \Phi(t, L) = -G \Gamma \partial_s \Phi(t, L) + F(\partial_t \Phi(t, L)), \end{cases} \quad (2.10)$$

c is a constant wave speed: $c = \sqrt{G/\rho}$, L is the bit position with respect to the s axis, $F(\partial_t \Phi(t, L))$ the reaction frictional torque at the bit and $G \Gamma \partial_s \Phi(t, L)$ is

the contact torque along the drillstring, (here $\partial_s = \partial()/\partial s$ is the derivation with respect to s). In this work, the authors reduce the study of the model to the study of the associated neutral differential equation for which they establish an analytical linearized stability criterion and give some numerical bifurcation elements. Certainly, the infinite dimensional aspect of the above model is adequate for describing the drilling process, but ignoring the axial vibrations and their influence on the global dynamics is disadvantageous when the aim is to establish a steadfast model.

A similar model but with different boundary conditions was already established in [35] and exploits the flatness property of the wave equation for suppressing the stick-slip undesired dynamics. Indeed, the author proves that the use of the top velocity measures ensures the control and the stabilization of the torsional vibrations.

The contribution [17] is worth mentioning, where a wave equation with different boundary conditions is used to model torsional vibrations for which the authors establish ultimate bounds for a distributed drill pipe model. The result is obtained through an analysis based on a difference equation model and on a wave equation description achieved through the direct Lyapunov method.

Next, in [33] as well as in [18], the authors considered a simplified drillstring model which describes not only the torsional vibration but also the axial one:

$$\begin{cases} I \frac{d}{dt^2} \Phi(t) + C(\Phi(t) - \Omega t) = -T(t), \\ M \frac{d}{dt^2} U(t) = W_0 - W(t). \end{cases} \quad (2.11)$$

The variables U and Φ denote the vertical and the angular positions of the drag bit, respectively. The reacting weight-on-bit $W(t)$ originates from the process of rock destruction occurring at the bit-rock interface and $T(t)$ is the reacting torque-on-bit. The stick-slip dynamics is numerically studied in [33] and in [18] a nonlinear analytical study is conducted for a simple frictional weight and torque proportional to $1 + \text{sign}(dU/dt)$. On the one hand, the model depicted in (2.10) neglects axial vibrations and on the other hand the lumped model (2.11) loses the infinite dimensional character of a PDE model.

In [41], the authors consider a PDE modeling the torsional vibrations and propose a mechanism called torsional rectification and compare it with existing soft-torque devices through a series of mathematical models. Both analytic and numerical simulations indicate that many of the volatilities suffered by existing soft-torque feedback approaches used to avoid slip-stick can be eliminated by their proposed alternative. Ignoring the axial vibrations and their influence on the torsional dynamics is disadvantageous since the study concerns exclusively the control of torsional vibrations.

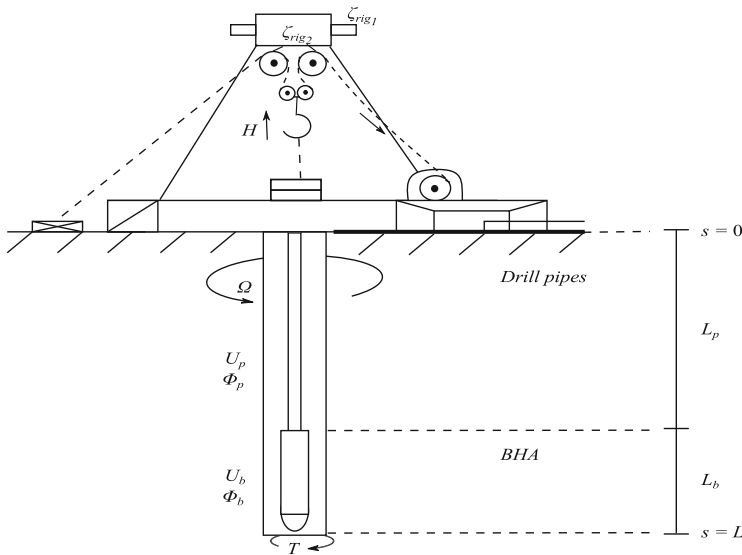


Fig. 2.3 Simplified scheme depicting an oilwell rotary drilling system

2.5 A System-Oriented Approach: Interconnected Dynamics

We aim at presenting an improved partial differential equations model with more realistic coupled nonlinear boundary conditions. This model takes into account the axial and torsional vibrations along the drilling system. Furthermore, an adjustable three dependent parameters analytic model is taken for the torque on bit. The proposed friction law is a nonlinear function allowing to continuously reproduce classical empirical friction profiles. Moreover, the established physical model can be transformed into a *time-delay system*. This fact is noteworthy since the measurement of the bit state is delayed, due to technological constraints. In our opinion, this is thus a natural way to design a model with unified structure.

The description of the considered model governing the mechanical axial/torsional vibrations follows.

2.5.1 Drillstring Mechanics

Denoting by U the axial vibrations and by Φ the torsional vibrations, the improved model is Fig. 2.3:

$$\begin{cases} \partial_t^2 U(t, s) = c^2 \partial_s^2 U(t, s), \\ E \Gamma \partial_s U(t, 0) = \alpha_1 \partial_t U(t, 0) - \alpha_2 H(t), \\ M \partial_t^2 U(t, L) = -E \Gamma \partial_s U(t, L) + F(\partial_t U(t, L)), \end{cases} \quad (2.12)$$

and

$$\begin{cases} \partial_t^2 \Phi(t, s) = \tilde{c}^2 \partial_s^2 \Phi(t, s), \\ G \Sigma \partial_s \Phi(t, 0) = \beta_1 \partial_t \Phi(t, 0) - \beta_2 \Omega(t), \\ J \partial_t^2 \Phi(t, L) = -G \Sigma \partial_s \Phi(t, L) + \tilde{F}(\partial_t U(t, L)). \end{cases} \quad (2.13)$$

Here G is the shear modulus of the drillstring steel and E the Young's elasticity modulus. Then, the wave speeds can be expressed by $c = \sqrt{E/\rho}$ and $\tilde{c} = \sqrt{G/\rho}$. The inertia $J = M r^2$ where r is taken as the averaged radius of the drill pipes, Γ is the averaged section of the drill pipes and Σ is the quadratic momentum. The nonlinear nature of the model is considered by taking appropriate models of the friction profiles F and \tilde{F} of the form: $z \mapsto pkz/(k^2 z^2 + \zeta)$, where the parameters k, ζ ($0 < \zeta \ll 1$ and $0 < k < 1$) are positive integers responsible of the sharpness of the friction force function and p is acting on its amplitude, see [6, 7]. Moreover, the behavior of the chosen friction model is close from the empirical model (the white friction force) but its smoothness is very useful in experimental identifications.

The contributions of the proposed model can be summarized as follows:

- **Infinite-dimensional setting for modeling:** As emphasized by (2.12)–(2.13), each type of vibrations is described by a PDE. The first equation of (2.12) means that axial vibrations U are governed by a wave equation with velocity c . In the second equation of (2.12), the reacting force due to the drillstring at the top is seen as the difference between the imposed vertical upward force and the actual drillstring friction force of viscous type at the top $\alpha \partial_t U(t, 0)$. The second equation of (2.12) describes a behavior equation sampled at the top of the hole. It simply expresses that the difference between the H the brake motor control (upward hook force) and the force generated by the gradient of the axial vibration at the top $\alpha \partial_s U(t, 0)$ is nothing else than a friction force of viscous type $\alpha \partial_t U(t, 0)$. Furthermore, for equation (2.13), torsional vibrations are also assumed to obey to a wave equation with velocity \tilde{c} . In the second equation of (2.13) the right hand side describes the difference between the motor speed and angular velocity of the first pipe. Finally, the third equation of (2.12) and (2.13) are established by applying the Fundamental Laws of Motion [1] at the bit.
- **Coupled dynamics:** The third equation of (2.13) generates the interconnection between the two dynamics. Indeed, it is generally recognized that the torque on bit, which is the main generator for friction in the drilling torsional vibrations, is expressed as a function of the axial vibration (see for instance [19]).
- **Nonlinear dynamics:** Both of the functions F and \tilde{F} are assumed to be nonlinear functions allowing to reproduce continuously the classical empirical friction profile.

2.5.2 Actuating Part and Motor Types

The drilling system includes three motors, which convert electrical energy into mechanical energy: one for the rotary table, one for the drawworks, and one for the mud pump, yielding three control variables. Each machine is modeled by a system of mechatronic equations as follows. The motor types have to be quite resistant, wherefrom the following choices.

DC motor. A first type of motor is the direct current armature control motor. The torque developed by the motor is proportional to the stator's flux and the current in the armature and we have $\Gamma = k_f \psi K_a I$ where Γ is the shaft torque, ψ is the magnetic flux in the stator field, which is assumed to be constant, I is the current in the motor armature. Since the flux is maintained constant, we can also write $\Gamma = k_T I$ where $k_T = k_f \psi K_a$.

When a current carrying conductor passes through a magnetic field, a voltage V_b appears, corresponding to the so-called back electromagnetic force $V_b = k_e \omega$ where ω is the rotation speed of the motor shaft. The constant k_T and k_e have the same value. Kirchhoff's law yields the electronic equation of the motor:

$$V - V_{res} - V_{coil} - V_b = 0, \quad (2.14)$$

where V is the input voltage, $V_{res} = -R I$ the armature resistor voltage (R being the armature resistor), $V_{coil} = L \dot{I}$ the armature inductance voltage (L being the armature inductance). The motor's electrical equation is then

$$L \dot{I} = -k_e \omega - R I + V. \quad (2.15)$$

Induction motor. A second type of motor is the induction machine. When AC current is applied to such a machine, the rotating magnetic field is set up in the stator. This rotating field is moving with respect to the rotor windings and thus induces a current flow in the rotor. The current flowing in the rotor windings sets up its own magnetic field. In the stationary reference frame ($\omega_s = 0$) the stator voltage vector can be expressed as $v_s^S = R_s i_s^S + \dot{\psi}_s^S$ where i_s^S and ψ_s^S are the stator current and rotor flux vectors. In the same way the rotor voltage vector can be expressed in the rotor fixed reference frame rotating with ω_R : $v_r^R = R_r i_r^R + \dot{\psi}_r^R$, whereas i_r^R and ψ_r^R are the rotor current and rotor flux vectors. The transformation in an arbitrary reference frame rotating with ω_k yields:

$$\begin{cases} v_s^k = R_s i_s^k + \dot{\psi}_s^k + j p \omega_k \psi_s^k \\ v_r^k = R_r i_r^k + \dot{\psi}_r^k + j p (\omega_k - \omega_r) \psi_r^k. \end{cases} \quad (2.16)$$

The flux vectors may be expressed as:

$$\begin{cases} \psi_s^k = L_s i_s^k + L_m i_r^k \\ \psi_r^k = L_r i_r^k + L_m i_s^k. \end{cases} \quad (2.17)$$

In the following the so-called D/Q-reference frame which is aligned to the rotor flux vector will be used and the superscript will be omitted, i.e. $\psi_r = \psi_{rd} + j\psi_{rq} = \psi_r^s e^{-j\rho}$, whereas ρ is the rotor flux angle in the stationary reference frame. Substituting the stator flux and rotor current vectors in (2.16) using (2.17) and introducing $\eta = 1 - (L_m^2/L_s L_r)$, $\chi = L_m^2 R_r / \sigma L_s L_r^2 + R_s / \sigma L_s$, $\zeta = R_r / L_r$ and $\xi = L_m / \sigma L_s L_r$. To further simplify the notations, we shall set: $I_{sd} = I_d$, $I_{sq} = I_q$, the stator current components in the D/Q reference frame, $\psi_{rd} = \psi_d$ the rotor flux D component, $v_{sd} = v_d$, $v_{sq} = v_q$ the stator voltage components in the D/Q reference frame.

We thus obtain conclude with the description of the induction machine model: its electric model and its mechanical model which respectively consist of four and a two dimensional nonlinear system. Indeed, the current/flux equations are given by

$$\begin{cases} \dot{\psi}_d = -\zeta(\psi_d - L_m I_d) \\ \dot{\rho} = p\omega_R + \zeta L_m \frac{I_d}{\psi_d} \\ \dot{I}_d = -\chi I_d + \zeta \xi \psi_d + p\omega_R I_q + \zeta L_m \frac{I_q^2}{\psi_d} + \frac{v_d}{\eta L_s} \\ \dot{I}_q = -\chi I_q - p\xi \omega_R I_d - \zeta L_m \frac{I_q I_d}{\psi_d} + \frac{v_q}{\eta L_s} \end{cases}, \quad (2.18)$$

and the mechanical model is defined by

$$\begin{cases} J\dot{\omega}_R = \mu\psi_{rd}I_{sq} - T_l \\ \dot{\theta}_R = \omega_R, \end{cases} \quad (2.19)$$

whereas $\mu = 3pM/2L_r$ and θ_R is the rotor angle and T_l the load torque.

2.6 Integration into a More Complete Traction-Compression/Torsional Model

2.6.1 Step by Step Description

A more complete model can be established by considering the BHA length and vibrations, neglected in the previous model. Thus, the length of the drillstring L

denotes $L_p + L_b$ where L_p is the pipes length and L_b is the BHA length. Here, the vibrations along the pipes will be distinguished from the ones along the BHA. Thus the model for axial vibrations U_p and torsional vibrations Φ_p along the pipes and axial vibrations U_b and torsional vibrations Φ_b along the BHA are governed by the system of PDE (2.20)–(2.27).

Pipe Drillstring The pipe drillstring deformation is modelled through a wave equation with both internal viscoelastic Kelvin-Voigt damping, and simple viscous damping:

$$\begin{cases} \rho A_p \partial_t^2 U_p(t, s) = E A_p \partial_s^2 U_p(t, s) + \varepsilon_{U_p}^i \partial_t \partial_s U_p(t, s) + \gamma_{U_p}^v \partial_t U_p(t, s) \\ \rho J_p \partial_t^2 \Phi_p(t, s) = G J_p \partial_s^2 \Phi_p(t, s) + \varepsilon_{\Phi_p}^i \partial_t \partial_s \Phi_p(t, s) + \gamma_{\Phi_p}^v \partial_t \Phi_p(t, s), \end{cases} \quad (2.20)$$

where $0 < s < L_p$, the internal damping coefficients are $\varepsilon_{U_p}^i$, $\varepsilon_{\Phi_p}^i$, and the viscous damping coefficients are $\gamma_{U_p}^v$, $\gamma_{\Phi_p}^v$. Additionally, ρ is the steel density, E (resp. G) denotes Young's (resp. the shear) modulus of drillstring steel, and A_p , J_p are the cross-section and polar inertia moment of one section, given by:

$$A_p = \pi(r_{po}^2 - r_{pi}^2), \quad J_p = \frac{\pi}{2} (r_{po}^4 - r_{pi}^4),$$

with r_{pi} and r_{po} the inner and outer pipe radius.

Top Boundary Conditions At $s = 0$, we consider the following boundary condition for Φ_p :

$$J_{top} \partial_t^2 \Phi_p(t, 0) = G J_p \partial_s \Phi_p(t, 0) + u_T(t), \quad (2.21)$$

with J_{top} the top drive inertia, and u_T the torque produced by the rotary table motor, taken as a *control input*. which is a more realistic boundary condition compared to the one in [2, 19]: $\Phi_p(t, 0) = \Omega_0 t$. Note that Eq. (2.21) can also be completed by the mechanical equation of an induction machine in place of (2.19).

The upward force H acts in the top hole device composed mainly of the derrick, the crown block and the traveling block. This whole setting is modeled as a two coupled mass spring system, following [32]

$$\begin{cases} M_{rg1} \ddot{\zeta}_{rg1}(t) + \gamma_{rg1} \dot{\zeta}_{rg1}(t) + M_{rg1} g = u_F(t) + k_{rg12} (\zeta_{rg2}(t) - \zeta_{rg1}(t)) - k_{rg01} \zeta_{rgini}(t) \\ M_{rg2} \ddot{\zeta}_{rg2}(t) + \gamma_{rg2} \dot{\zeta}_{rg2}(t) + M_{rg2} g = -H(t) - k_{rg12} (\zeta_{rg2}(t) - \zeta_{rg1}(t)). \end{cases} \quad (2.22)$$

Here, ζ_{rg1} accounts for vibrations in all drilling rig elements except the drilling string, BHA, cables, drawworks, travelling and crown blocks ; ζ_{rg2} accounts for elasticity in cables, crown and travelling blocks ; the effort $k_{rg01} \zeta_{rgini}$ represents the ground reaction force and $u_F(t) = k_{rg01} (\zeta_{rg1}(t) - \zeta_{rg0}(t))$ is a tension force in the cable at the drawworks level, taken as a *control input* (being directly related to the drawworks rotation motor). The parameters M_{rgi} , γ_{rgi} and k_{rgij} are equivalent masses, damping coefficients and stiffness coefficients, respectively.

For U_p consider the boundary condition at $s = 0$:

$$M_{top} \partial_t^2 U_p(t, 0) = E A_p \partial_s U_p(t, 0) + H(t). \quad (2.23)$$

with M_{top} the top drive mass. In [19], a simpler boundary condition is adopted: $E A_p \partial_s U_p(t, 0) = H(t)$. The initial conditions are taken such that $\Phi_p, \partial_t \Phi_p, \partial_s \Phi_p, U_p, \partial_t U_p, \partial_s U_p$ vanish at $t = 0$.

Drill Collars The BHA equations for axial vibrations U_b and torsional vibrations Φ_b are given by

$$\begin{cases} \rho A_b \partial_t^2 U_b(t, s) = G A_b \partial_s^2 U_b(t, s) + \varepsilon_{U_b}^i \partial_t \partial_s U_b(t, s) + \gamma_{U_b}^v \partial_t U_b(t, s) \\ \rho J_b \partial_t^2 \Phi_b(t, s) = E J_b \partial_s^2 \Phi_b(t, s) + \varepsilon_{\Phi_b}^i \partial_t \partial_s \Phi_b(t, s) + \gamma_{\Phi_b}^v \partial_t \Phi_b(t, s), \end{cases} \quad (2.24)$$

where $L_p < s < L$, and A_b, J_b are, as above, the cross-section and polar inertia moment of one section, given by

$$A_b = \pi(r_{bo}^2 - r_{bi}^2), \quad J_b = \frac{\pi}{2} (r_{bo}^4 - r_{bi}^4),$$

with r_{bi} and r_{bo} are inner and outer drill collar radius.

Pipe/Drill Collar Continuity Conditions To achieve continuity in speed and effort, Φ_p, Φ_b, U_b and U_p satisfy the connexion conditions:

$$\begin{cases} \partial_t \Phi_b(t, L_p) = \partial_t \Phi_p(t, L_p) \\ \partial_s \Phi_b(t, L_p) = \frac{J_p}{J_b} \partial_s \Phi_p(t, L_p) \\ \partial_t U_b(t, L_p) = \partial_t U_p(t, L_p), \\ \partial_s U_b(t, L_p) = \frac{A_p}{A_b} \partial_s U_p(t, L_p), \end{cases} \quad (2.25)$$

where J_* and A_* are $J_* = \pi(r_{*o}^4 - r_{*i}^4)/2$ and $A_* = \pi(r_{*o}^2 - r_{*i}^2)$.

Bottom Hole Boundary Conditions The boundary conditions at $s = L$ for torsional vibrations Φ_b are

$$J_{bit} \partial_t^2 \Phi_b(t, L) = -G J_b \partial_s \Phi_p(t, L) + T_{bit}(t), \quad (2.26)$$

where T_{bit} is the reaction torque at the bit. For axial vibrations, the bottom boundary condition is

$$M_{bit} \partial_t^2 U_b(t, L) = -E A_b \partial_s U_p(t, 0) + W_{bit}(t). \quad (2.27)$$

where M_{bit} is the bit's mass, and $W_{bit}(t)$, the reaction force at the bit due to the so called dynamic weight on bit (DWOB).

Forces/Moments Expressions The bottom hole force and moment can be decomposed into a cutting and a frictional part

$$T_{bit} = T_c + T_f, \quad W_{bit} = W_c + W_f, \quad (2.28)$$

Friction Force/Moment. The expressions for T_f and W_f are taken as (see for instance [19, 31]):

$$T_f(t) = \frac{a^2}{2} \gamma \mu \sigma l \mathcal{F}(\|V_b(L, t)\|), \quad W_f(t) = a l \sigma \mathcal{F}(\|V_b(L, t)\|),$$

where a is the bit radius, l the length of the wearflat, σ the contact stress, γ accounts for the distribution and orientation of the frictional forces acting at the wearflat/rock interface, μ the ratio between the horizontal and the vertical components of the frictional force, $V_b = (\partial_t U_p, \partial_t \Phi_p)$ and $\text{sgn}(V_b)$ designate the orientation of V_b with respect to the horizontal plane, and \mathcal{F} is an adimensional friction function. We consider the following expressions for such an \mathcal{F} , as for instance in [31]

$$\mathcal{F}(r) = \frac{\alpha r}{\sqrt{r^2 + \varepsilon^2}}, \quad (2.29)$$

or in [42]

$$\mathcal{F}(r) = \beta \left(\tanh(r) + \frac{\gamma_1}{1 + \gamma_2 r^2} \right). \quad (2.30)$$

Cutting Force/Moment. The expressions for T_c and W_c are taken as (see e.g. [19]):

$$T_c(t) = \frac{a^2}{2} \varepsilon d(t), \quad W_c(t) = a \zeta \varepsilon d(t),$$

where a is the bit radius, d the depth of cut, ε is the intrinsic specific energy, and ζ the ratio of the vertical to the horizontal force for a sharp cutter. Here the cut depth $d(t)$ is deduced from the relation

$$d(t) = n(U_b(t, L) - U_b(t - t_n, L)), \quad (2.31)$$

where n is the bit number of blades and t_n is implicitly given through the relation

$$\frac{2\pi}{n} = \Phi_b(t, L) - \Phi_b(t - t_n, L). \quad (2.32)$$

The range of t_n is given by $t_{n_0} = 2\pi/(n\Omega_0)$, with Ω_0 a nominal rotating speed at the top. Note that, in [31], T_c is defined by:

$$T_c(t) = -a_4(\mathcal{F}(\|V_b(L, t)\|))^2 d(t). \quad (2.33)$$

2.6.2 Full Model Summary

Let us rewrite the previous model in a more compact form.

Pipe Drillstring Pipes wave equation (torsion—traction/compression)

$$\rho A_p \partial_t^2 U_p(t, s) = E A_p \partial_s^2 U_p(t, s) + \varepsilon_{U_p}^i \partial_t \partial_s U_p(t, s) + \gamma_{U_p}^v \partial_t U_p(t, s), \quad (2.34a)$$

$$\rho J_p \partial_t^2 \Phi_p(t, s) = G J_p \partial_s^2 \Phi_p(t, s) + \varepsilon_{\Phi_p}^i \partial_t \partial_s \Phi_p(t, s) + \gamma_{\Phi_p}^v \partial_t \Phi_p(t, s). \quad (2.34b)$$

Top Boundary Conditions Induction motor (torsion):

$$\dot{\psi}_{\Phi d} = -\zeta_{\Phi}(\psi_{\Phi d} - L_{\Phi m} I_d) \quad (2.35a)$$

$$\dot{\rho}_{\Phi} = p\omega_{\Phi R} + \zeta_{\Phi} L_{\Phi m} \frac{I_{\Phi d}}{\psi_{\Phi d}} \quad (2.35b)$$

$$\dot{I}_{\Phi d} = -\chi_{\Phi} I_{\Phi d} + \zeta_{\Phi} \xi_{\Phi} \psi_{\Phi d} + p_{\Phi} \omega_{\Phi R} I_{\Phi q} + \zeta_{\Phi} L_{\Phi m} \frac{I_{\Phi q}^2}{\psi_{\Phi d}} + \frac{v_{\Phi d}}{\eta_{\Phi} L_{\Phi s}} \quad (2.35c)$$

$$\dot{I}_{\Phi q} = -\chi_{\Phi} I_{\Phi q} - p_{\Phi} \xi_{\Phi} \omega_{\Phi R} I_{\Phi d} - \zeta_{\Phi} L_{\Phi m} \frac{I_{\Phi q} I_{\Phi d}}{\psi_{\Phi d}} + \frac{v_{\Phi q}}{\eta_{\Phi} L_{\Phi s}}. \quad (2.35d)$$

Drill pipes top boundary condition (torsion):

$$J_{top} \partial_t^2 \Phi_p(t, 0) = G J_p \partial_s \Phi_p(t, 0) + u_T(t). \quad (2.36)$$

Induction motor (traction/compression):

$$\dot{\psi}_{Ud} = -\zeta_U(\psi_{Ud} - L_{Um} I_d) \quad (2.37a)$$

$$\dot{\rho}_U = p\omega_{UR} + \zeta_U L_{Um} \frac{I_{Ud}}{\psi_{Ud}} \quad (2.37b)$$

$$\dot{I}_{Ud} = -\chi_U I_{Ud} + \zeta_U \xi_U \psi_{Ud} + p_U \omega_{UR} I_{Uq} + \zeta_U L_{Um} \frac{I_{Uq}^2}{\psi_{Ud}} + \frac{v_{Ud}}{\eta_U L_{Us}} \quad (2.37c)$$

$$\dot{I}_{Uq} = -\chi_U I_{Uq} - p_U \xi_U \omega_{UR} I_{Ud} - \zeta_U L_{Um} \frac{I_{Uq} I_{Ud}}{\psi_{Ud}} + \frac{v_{Uq}}{\eta_U L_{Us}}. \quad (2.37d)$$

Top hole assembly (traction/compression):

$$M_{rg1} \ddot{\zeta}_{rg1}(t) + \gamma_{rg1} \dot{\zeta}_{rg1}(t) + M_{rg1} g = u_F(t) + k_{rg12}(\zeta_{rg2}(t) - \zeta_{rg1}(t)) - k_{rg01} \zeta_{rgini}(t) \quad (2.38a)$$

$$M_{rg2} \ddot{\zeta}_{rg2}(t) + \gamma_{rg2} \dot{\zeta}_{rg2}(t) + M_{rg2} g = -H(t) - k_{rg12}(\zeta_{rg2}(t) - \zeta_{rg1}(t)). \quad (2.38b)$$

Drill pipes top boundary condition (traction/compression):

$$M_{top} \partial_t^2 U_p(t, 0) = EA_p \partial_s U_p(t, 0) + H(t). \quad (2.39)$$

Drill Collars

$$\rho A_b \partial_t^2 U_b(t, s) = GA_b \partial_s^2 U_b(t, s) + \varepsilon_{U_b}^i \partial_t \partial_s U_b(t, s) + \gamma_{U_b}^v \partial_t U_b(t, s), \quad (2.40a)$$

$$\rho J_b \partial_t^2 \Phi_b(t, s) = EJ_b \partial_s^2 \Phi_b(t, s) + \varepsilon_{\Phi_b}^i \partial_t \partial_s \Phi_b(t, s) + \gamma_{\Phi_b}^v \partial_t \Phi_b(t, s). \quad (2.40b)$$

Pipe/Drill Collar Continuity Conditions

$$\partial_t \Phi_b(t, L_p) = \partial_t \Phi_p(t, L_p) \quad (2.41a)$$

$$\partial_s \Phi_b(t, L_p) = \frac{J_p}{J_b} \partial_s \Phi_p(t, L_p) \quad (2.41b)$$

$$\partial_t U_b(t, L_p) = \partial_t U_p(t, L_p) \quad (2.41c)$$

$$\partial_s U_b(t, L_p) = \frac{A_p}{A_b} \partial_s U_p(t, L_p). \quad (2.41d)$$

Bottom Hole Boundary Conditions Drill collar bit boundary condition (torsion):

$$J_{bit} \partial_t^2 \Phi_b(t, L) = -G J_b \partial_s \Phi_p(t, L) + T_{bit}(t). \quad (2.42)$$

Drill collar bit boundary condition (traction/compression):

$$M_{bit} \partial_t^2 U_b(t, L) = -EA_b \partial_s U_p(t, 0) + W_{bit}(t). \quad (2.43)$$

Forces/Moments Expressions Bottom hole force and moment:

$$T_{bit} = T_c + T_f, \quad W = W_c + W_f. \quad (2.44)$$

Friction Force/Moment:

$$T_f(t) = \frac{a^2}{2} \gamma \mu \sigma l \mathcal{F}(\|V_b(L, t)\|), \quad W_f(t) = a l \sigma \mathcal{F}(\|V_b(L, t)\|).$$

Adimensional friction function expressions:

$$\mathcal{F}(r) = \frac{\alpha r}{\sqrt{r^2 + \varepsilon^2}} \quad \text{First expression} \quad (2.45)$$

$$\mathcal{F}(r) = \beta \left(\tanh(r) + \frac{\gamma_1}{1 + \gamma_2 r^2} \right) \quad \text{Second expression} \quad (2.46)$$

Cutting Force/Moment:

$$T_c(t) = \frac{a^2}{2} \varepsilon d(t), \quad W_c(t) = a \zeta \varepsilon d(t)$$

Cut depth $d(t)$ defined by $d(t) = n(U_b(t, L) - U_b(t - t_n, L))$.

One revolution duration t_n such that $\frac{2\pi}{n} = \Phi_b(t, L) - \Phi_b(t - t_n, L)$.

2.7 Wireless-Transmission and Real-Time Control Methodology

In this section, we focus on the way to bring the measurement from downhole to surface so we can use it in order to improve the observer/controller behavior. There are mainly three types of transmission: (i) through telemetry signals along the drilling fluid, often referred to as mud-pressure pulses, (ii) through acoustic waves along the drillstring [10], (iii) through wired drill pipes.

In most of the literature, electronic equipments are designed for data acquisition and for modulation purpose. It should be implemented as an autonomous system energized either by a mud operated electrical turbine or by a battery pack [39].

Mud-pulse telemetry This technology uses the mud that goes through the drilling system as a transmission media. The data will be represented by pressure pulses. According to [39], the pulser actuator (a stepper-motor-based device) and a main valve restricts the flow and creates some pressure-pulse sequence. A piezoelectric device captures these variations that are then analyzed by a micro-controller. Evidently, due to the irregular nature the mud flow, the low frequency vibrations produced by mud pumps and pulsation dampeners the signals are corrupted by noise. Furthermore, they have an important attenuation. Some characteristics to highlight are [10, 16, 23] its cost-effective data transfer, its very low bite rate (1 or 2 bits per second).

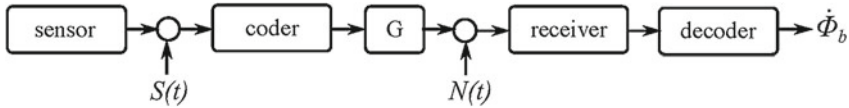


Fig. 2.4 Testbed schematics with sonar pulses

Mud-pulse velocity declines with the disturbances of mud density, gas content and mud compressibility. It becomes more difficult with increasing well depth. Pulse waves travel through the borehole at 1200 m/s [23], hence the measure arrives with some delay that increases up to $\tau_{max} \approx 6.6$ s.

Acoustic data transmission over a drill string Since the acoustic wave propagation velocity in the string material is at least three times superior to that in the mud of the borehole [10], and a higher transmission rate is possible (typically 6 bps), acoustic transmission seems to be the best way to emit pulses to the surface. These acoustic waves are generated by torsional contractions created by magneto restrictive rings set inside the pipe [15]. In this case $\tau_{max} \approx 2.2$ s. It is useful to note that there exists an attenuation of around 4 dB/300 m [14]. However, we can neglect it because there is always a possibility of setting a repeater at any joint at each 10–15 m of the section. We consider that this fact does not add any extra considerable delay since the repeater's amplification can occur almost instantaneously.

The telemetry system sends signals directly to the surface through the channel. Usually, there is an embedded sensor measuring $\dot{\phi}_b$ downhole. A measurement noise $S(t)$ is added to the data and then coded all together, so that it can be transmitted through the acoustic channel G . At surface, a receiver will read the encoded signal with the noise $N(t)$. Furthermore, a digital algorithm is used to decode this data and make it available for the use for further treatments. Both methods can be modeled by the schematic as shown in Fig. 2.4. On the bit state measurement side, there are mainly three types of transmission:

Transmission delay range and friction hypothesis Due to technical considerations we can assume that the transmission media is, as a first approximation, like a pure delay system with delay time $\tau \in [0, \tau_{max}]$. Moreover, the well's depth increases at a very slow rate and it stops each 10–15 m. In this procedure, the delay can be recalculated. Hence, the delay can be defined as a constant, that is $\dot{\tau} = 0$.

On the other hand, we will consider that the friction coefficient is constant or at least slow time variant $\dot{\tau} \approx 0$. This approximation is often assumed in the context of adaptive control. This hypothesis means that the rate of variation of the rock friction coefficient does not exhibit substantial changes during drill-operation. Even if the drilled surfaces may have different friction characteristics, the rate of penetration remains small ($\dot{d} \approx 0$).

Real-time control The general real time control architecture has to handle output signal transmission, state observation under variable delay and signal noises presence as well as the state feedback control calculation and actuation update. A detailed description of a such an architecture is given in [3] where more emphasis is put on observer performance in presence of transmission delay variations, noise perturbation and friction coefficient variation. Due to these parameter variation the overall observer/controller order is increased which has to be considered in the specification of real time control architecture. We will not go further in the specification and the design of overall real time communication and calculation architecture which is out of the scope of this work, but it is important to emphasize the fact that the reliability, bandwidth and signal to noise ratio of data transmission channel is of great importance in the quality of state observation and control.

2.8 Concluding Remarks:

The complete description of a Drilling oilwell machine involves three interconnected systems: (i) A mechanical system, more precisely, the drillstring that is the down-hole part of the drilling device, (ii) The mechatronic system: composed mainly from two induction machines: the first acting axially and the second acting in rotation, (iii) A transmission system that consists from sensors (piezoelectric) and a transmission vector that can be for instance the wireless technology.

Briefly, the interconnection of such components can be summarized as follows: The drillstring and the induction machine are connected via the derrick, the crown and the traveling block for the axial actions and via the rotary table for angular rotation. Moreover, the induction motors are the only actuators leading to the control for guaranteeing a regular drilling process. The success of such a task lies mainly on the bit-data (the mechanical system) furnished by the sensors and transmitted by wireless to the top. The transmitted data are then responsible on the motor actions.

Finally, it is worthy to note that the preceding model does not take into account the bending vibrations (leading to whirling) of the drilling collar, nor the drilling fluid dynamics.

Appendix: Notations table

Variable	Signification
L_p	Pipe length
L_b	Bor Hole Assemble length
L	$= L_p + L_b$
U_p, U_b	Pipe, drill collar traction/compression deformation
Φ_p, Φ_b	Pipe, drill collar torsional deformation
$\varepsilon_{U_p}^i, \varepsilon_{\Phi_p}^i$	Internal damping coefficients
$\gamma_{U_p}^v, \gamma_{\Phi_p}^v$	Viscous damping coefficients
ρ	Steel density
E, G	Young's, shear modulus of drillstring steel
A_p, J_p	Cross-section and polar inertia moment of one pipe section
A_b, J_b	Cross-section and polar inertia moment of one drill collar section
r_{po}, r_{pi}	Outer, inner pipe radius
r_{bo}, r_{bi}	Outer, inner drill collar radius
$\Psi_{\phi_d}, \Psi_{U_d}$	D component of rotary table (torsion) induction motor flux
L_{ϕ_m}, L_{U_m}	Torsion, traction/compression induction motor mutual inductance
I_{ϕ_d}, I_{ϕ_q}	D, Q component of stator current in torsion induction motor
I_{U_d}, I_{U_q}	D, Q component of stator current in traction/compression induction motor
J_{Iop}	Top drive inertia
u_T	Rotary table motor torque, taken as a <i>control input</i>
H	Force acting in the top hole device
ζ_{rg1}	Accounts for vibrations in all drilling rig elements except the drilling string, BHA, cables, drawworks, travelling and crown blocks
ζ_{rg2}	Accounts for elasticity in cables, crown and travelling blocks
k_{rg01}, ζ_{rgini}	Ground reaction force
$u_F(t)$	$= k_{rg01}(\zeta_{rg1}(t) - \zeta_{rg0}(t))$, tension force in the cable at the drawworks level, taken as a <i>control input</i>
$M_{rgi}, \gamma_{rg1}, k_{rgij}$	Equivalent masses, damping coefficients and stiffness coefficients
M_{Iop}	Top drive mass
U_b, Φ_b	axial, torsional vibrations
T_{bit}	Bit reaction torque
M_{bit}	Bit's mass
$W_{bit}(t)$	Reaction force at the bit
T_c, W_c	Bottom hole cutting torque and force
T_f, W_f	Bottom hole friction torque and force
a	Bit radius
l	Length of the wearflat
σ	Contact stress
γ	accounts for the distribution and orientation of the frictional forces acting at the wearflat/rock interface
μ	Ratio between the horizontal and the vertical components of the frictional force
V_b	$= (\partial_t U_p, \partial_t \Phi_p)$
$\text{sgn}(V_b)$	designate the orientation of V_b with respect to the horizontal plane
\mathcal{F}	Adimensional friction function
d	Depth of cut
ε	Intrinsic specific energy
ζ	Ratio of the vertical to the horizontal force for a sharp cutter
n	Bit blade number

References

1. R. Abraham, J.E. Marsden, *Foundations of Mechanics* (The Benjamin/Comings Publishing, 1978)
2. A.G. Balanov, N.B. Janson, P.V.E. McClintock, C.H.T. Wang, Bifurcation analysis of a neutral delay differential equation modelling the torsional motion of a driven drill-string. *Chaos, Solitons Fractals* **15**, 381–394 (2002)
3. R. Barreto Jijon, C. Canudas-de-Wit, S.-I. Niculescu, J. Dumon, Adaptive observer design, under low data rate transmission with applications to oil well drill-string, in *American Control Conference*, (Baltimore, Maryland, USA, 2010)
4. D.A.W. Barton, B. Krauskopf, R.E. Wilson, Nonlinear dynamics of torsional waves in a drill string model with spacial extent. *J. Vibr. Control* **16**, 1049–1065 (2007)
5. I. Boussaada, H. Mounier, S.-I. Niculescu, A. Cela, I. Ciril, K. Trabelsi, Dynamics analysis of a Drillstring model. *SIAM Conference on Control and Its Applications* (2011)
6. I. Boussaada, H. Mounier, S.-I. Niculescu, A. Cela, in *Analysis of Drilling vibrations: A Time-Delay System Approach The 20th Mediterranean Conference on Control and Automation, MED 2012* (Barcelona, Spain, 2012), pp. 1–5
7. I. Boussaada, A. Cela, H. Mounier, S.-I. Niculescu, *Control of Drilling vibrations: A Time-Delay System-Based Approach, 11th IFAC Workshop on Time Delay Systems* (Grenoble, France, 2013)
8. C. Canudas-de Wit, F. Rubio, M. Corchero, D-oskil: a new mechanism for controlling stick-slip oscillations in oil well drillstrings. *IEEE Trans. Control Syst. Technol* **16**(6), 1177–1191 (2008)
9. N. Challamel, Rock Destruction effect on the stability of a drilling structure. *J. Sound Vibr.* **233**(2), 235–254 (2000)
10. F. Clayer, H. Heneusse, J. Sancho, Procédé de transmission acoustique de données de forage d'un puits. in *World Intellectual Property Organization*, March 1992. No. WO 92/04644 (In French)
11. F. Collado, B. D'Andréa-Novel, M. Fliess, H. Mounier, Rock Destruction effect on the stability of a drilling structure. *XXIIe Colloque GRETSI* **1–4** (2009)
12. E. Detournay, T. Richard, M. Shepherd, Drilling response of drag bits : theory and experiment. *J. Rock Mech. Min. Sci.* **45**, 1347–1360 (2008)
13. E. Detournay, P. Defourny, A phenomenological model of the drilling action of drag bits. *Int. J. Rock Mech. Min. Sci.* **29**(1), 13–23 (1992)
14. D. Drumheller, Acoustical properties of drill strings. *J. Acoust. Soc. Am.* **85**(3), 1048–1064 (1989)
15. D. Drumheller, An overview of acoustic telemetry. Sandia Research Report, Sand-92-0677c, December 1992
16. D. Drumheller, S. Knudsen, The propagation of sound waves in drill strings. *J. Acoust. Soc. Am.* **97**(4), 2116–2125 (1995)
17. E. Fridman, S. Mondié, B. Saldívar, Bounds on the response of a drilling pipe model. *IMA J. Math. Control Inf.* **1–14** (2010)
18. C. Gernay, N. Van De Wouw, H. Nijmeijer, R. Sepulchre, Nonlinear drilling dynamics analysis. *SIAM J. Dyn. Syst.* **8**, 527–553 (2005)
19. C. Gernay, Modeling and Analysis of self-excited Drill Bit Vibrations. PhD dissertation, University of Liège, 2009
20. G.H. Golub, C.F. Van Loan, *Matrix Computations* (The Johns Hopkins University Press, Baltimore, 1983)
21. K. Gu, V.L. Kharitonov, J. Chen, *Stability of Time-Delay Systems* (Birkhauser, Boston, 2003)
22. A. Kyllingstad, G.W. Halsey, A study of stick/slip motion of the bit. *SPE Drill. Eng.* **3–4**, 369–373 (1988)
23. X. Liu, B. Li, Y. Yue, Transmission behavior of mud-pressure pulse along well bore. *J. Hydrodyn.* **19**(2), 236–240 (2007)

24. I. Lopez, H. Nijmeijer, Prediction and validation of the energy dissipation of a friction damper. *J. Sound Vibr.* **328**, 396–410 (2009)
25. H. Mounier, Propriétés structurelles des systèmes linéaires a retard : Aspects théorique et pratique. Thèse de l'Université Paris-Sud, 1995, 148pp
26. H. Mounier, P. Rouchon, J. Rudolph, Some examples of linear systems with delays. *JESA-APII-RAIRO* **31**(6), 911–925 (1997)
27. E.M. Navarro-López, D. Cortés, Sliding-mode control of a multi-dof oilwell drillstring with stick-slip oscillations, in *American Control Conference* (2007), pp. 3837–3842
28. E.M. Navarro-López, R. Suárez, Practical approach to modelling and controlling stick-slip oscillations in oilwell drillstring, in *IEEE, International Conference on Control Applications* (2004), pp. 3162–3174
29. E.M. Navarro-López, R. Suárez, Modelling and analysis of stick-slip behavior in a drillstring under dry friction. *Congreso anual de la AMCA* **2004**, 330–335 (2004)
30. E.M. Navarro-López, An alternative characterization of bit-sticking phenomena in a multi-degree-of-freedom controlled drillstring. *Nonlinear Anal. Real World Appl.* **10**(5), 3162–3174 (2009)
31. S. Parfitt, R.W. Tucker, C. Wang, Drilling guidlines from the cosserat dynamics of a drill-rig assembly. preprint (2000)
32. D. Pavone, J.P. Desplans, Analyse et Modélisation du comportement dynamique d'un rig de forage. IFP report **42208** (1996)
33. T. Richard, C. Germay, E. Detournay, A simplified model to explore the root cause of stick-slip vibrations in drilling system with drag bits. *Appl. Math. Comput.* **305**, 432–456 (2007)
34. I. Rey-Fabret, J.F. Nauroy, O. Vincké, Y. Peysson, I. King, H. Chauvin, F. Cagnard. Intelligent drilling surveillance through real time diagnosis. *Oil Gas Sci. Technol. Rev. IFP* **59**(4), 357–369 (2004)
35. P. Rouchon, Flatness and stick-slip stabilization. *Tech. Rep.* **492**, 1–9 (1998)
36. B. Saldívar, S. Mondié, J.-J. Loiseau, V. Rasvan, Stick-slip oscillations in oilwell drillstrings: Distributed parameter and neutral type retarded model approaches, in *IFAC 18th World Congress Milano* (Italy) (2011), pp. 283–289
37. B. Saldívar, S. Mondié, Drilling vibration reduction via attractive ellipsoid method. *J. Franklin Inst.* **350**(3), 485–502 (2013)
38. B. Saldívar, S. Mondié, J.-J. Loiseau, V. Rasvan, Suppressing axial torsional coupled vibrations in oilwell drillstrings. *J. Control Eng. Appl. Inf.* **15**(1), 3–10 (2013)
39. P. Tubei, C. Bergeron, S. Bell, Mud-pulser telemetry system for down hole Measurement-While-Drilling, in *IEEE 9th Proceedings Instrument and Measurement Technology Conference* (1992), pp. 219–223
40. R.W. Tucker, C. Wang, Torsional vibration control and Cosserat dynamics of a drill-rig assembly. *Meccanica* **38**(1), 145–161 (2003)
41. R.W. Tucker, C. Wang, On the effective control of torsional vibrations in drilling systems. *J. Sound Vibr.* **224**(1), 101–122 (1999)
42. R.W. Tucker, C. Wang, The excitation and control of torsional slip-stick in the presence of axial vibrations. preprint (2000)

Recent Results on Time-Delay Systems
Analysis and Control

Witrant, E.; Fridman, E.; Sename, O.; Dugard, L. (Eds.)

2016, XI, 329 p. 55 illus., 34 illus. in color., Hardcover

ISBN: 978-3-319-26367-0